ACS APPLIED POLYMER MATERIALS

pubs.acs.org/acsapm

Article

Free-Standing Bacterial Cellulose/Polypyrrole Composites for Eco-Friendly Remediation of Hexavalent Chromium Ions

Radim Striz, Islam M. Minisy, Patrycja Bober, Oumayma Taboubi, Jiří Smilek, and Adriana Kovalcik*

Cite This: https://doi.org/10.1021/acsapm.4c00579

Read Online

ACCESS | Metrics & More | Article Recommendations | Supporting Information

ABSTRACT: Drinking water quality requirements are getting stricter but water sources are limited. Therefore, effective ways to purify it must be developed. In order to remove toxic Cr(VI) from wastewater, efficient, nontoxic, sustainable, resilient biocomposites based on bacterial cellulose (BC) and polypyrrole (PPy) have been fabricated. The free-standing BC/PPy composites, allowing easy handling during and after water treatment, were successfully prepared by the oxidative polymerization of pyrrole on the BC surface. The variation in the physical state of BC sheets used for coating by PPy was done to study the rheological properties and Cr(VI) removal capacity. Characterization techniques like FTIR, SEM, BET, thermogravimetric analysis, and rheological analyses established the morphology and structural properties of the prepared biocomposites. The physical state of the bacterial cellulose used for the coating by PPy positively affected the mechanical and thermal stabilities of the resulting BC/PPy composites but had almost no effect on the removal capacity of hexavalent chromium. The free-standing BC/PPy composites reached a specific surface area of 61.96 m^2 g^{-1} and a pore volume of 0.097 cm^3 g^{-1}, showing more than a threefold increase compared to neat BC sheets. The coating of BC by PPy markedly improved the maximum adsorption capacity of Cr(VI). The experimental Cr(VI) adsorption data fitted using Langmuir's isotherm model indicated homogeneous monolayer adsorption of Cr(VI) ions onto the BC/PPy surface. The Cr(VI) maximum adsorption capacity of BC/PPy composites was determined to be 294.1 mg g^{-1}. Furthermore, the BC/PPy composites were proved to be excellent catalysts for the photocatalytic reduction of toxic Cr(VI) into nontoxic Cr(III) ions. These results suggest that the free-standing BC/PPy composites could be used as alternative materials for eco-friendly remediation of hexavalent chromium ions from wastewater.

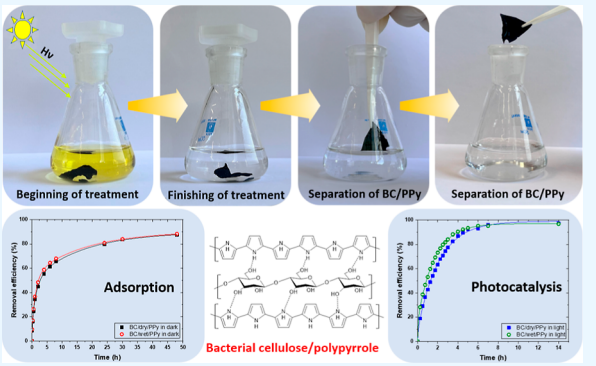

KEYWORDS: *bacterial cellulose, polypyrrole, composites, hexavalent chromium ions, reduction*

1. INTRODUCTION

Climate changes, rapid industrialization, urbanization, overpopulation, and excessive consumer behavior, all-encompassing a linear economy model, contribute to the scarcity of drinking water of the required quality.[1] The most widespread water pollutants include pesticides, fertilizers, pharmaceuticals, microplastics, dyes, coal, diesel phenols, and heavy metals.[2] Toxic compounds in water are undesirable and dangerous, mainly for living organisms.[3] The application of sustainable technologies for the remediation of heavy metals from water is essential to avoid serious environmental, economic, and social problems.[4] An example of a toxic heavy metal that has significant negative effects on human and animal health is hexavalent chromium, which is readily soluble in water. The toxic hexavalent chromium primarily coexists with relatively low-toxicity trivalent chromium. It was proved that Cr(III) does not penetrate cell membranes, unlike Cr(VI). The maximum value of total chromium in drinking water given by the WHO and the European Parliament is 50 μg L^{-1}, but since January 2036, it shall be 25 μg L^{-1} in the EU.[5,6] Numerous strategies with advantages and some limitations have been applied to remove Cr(VI) from water, including adsorption, membrane filtration, photocatalytic treatment, electrochemical treatment, microbiological treatment, flotation, and ion exchange.[7] Nowadays, in addition to the efficiency of the chosen method, sustainability without causing secondary pollution is also a criterion. From today's perspective, the materials used for water purification should fit into the concept of circular economy and green chemistry.[8]

Biopolymers and biocomposites with an adsorption capacity for water contaminants such as cellulose [including bacterial cellulose (BC)], lignin, starch, and chitosan are considered to be materials with enormous potential for water treatment.[9]

Received: February 23, 2024
Revised: May 2, 2024
Accepted: May 2, 2024

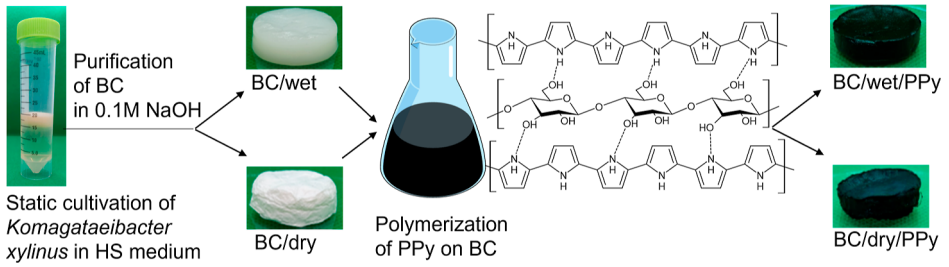

Figure 1. Schematic illustration of BC/PPy composites fabricated by PPy coating on BC and freeze-drying [color figure can be viewed in the online issue].

Their advantages include biodegradability, carbon neutrality, independence from fossil sources, and nontoxicity. The adsorption capacity of biopolymers can be further increased by various physical (e.g., surface area enhancement) and chemical modifications (e.g., functional group addition, cross-linking, and composite formation). Introducing additional functional groups like amino, carboxylic, and hydroxyl groups to natural adsorbent is especially effective to improve the interaction between biopolymers and metal ions as has been presented in several works.[10−12]

BC has all advantages of biomaterials, and, in addition, industrial waste can be used for biotechnological production.[13−15] BC is produced biotechnologically by *Komagataeibacter xylinus* as an extracellular polysaccharide.[16] The most productive BC production strain is considered *Komagataeibacter xylinus* (previously known as *Gluconacetobacter xylinus* or *Acetobacter xylinum*). The BC production yields depend on the strain,[17] culture medium,[18] and growing conditions.[19] BC is a nontoxic and biocompatible material formed by cellulose ribbon-like nanofibrils resembling nonwoven textile structures. In addition, it is a highly crystalline material with high mechanical flexibility and tensile strength. Due to the hydrogen bridges' content and many pores in the structure, BC can retain high amounts of water. Therefore, BC may be classified as a hydrogel.[20] Hydrogels with high adsorption capacity are attractive materials for wastewater treatment.[21] The application of BC for filtration and water treatment has been proposed as more effective after chemical modifications contributing to higher reactivity and adsorption capacity.[16]

This study focuses on the adsorption and removal efficiency of hexavalent chromium ions from water by a bioadsorbent based on BC and polypyrrole (PPy). PPy is one of the prominent conductive polymers with unique characteristics (e.g., a broad range of conductivity, electroactivity, polarizability, response-ability, and nontoxicity).[22] In addition, PPy has a high affinity for heavy metal ions and forms complexes with them.[22,23] It was shown that the PPy salt synthesized sonochemically in the powder form exhibited the adsorption capacity of Cr(VI) ions about 21.87 mg g^{-1} at a pH of 3.2 and 34 °C.[24] However, the direct use of PPy in its powder form is particularly problematic, regarding separation from wastewater. Few studies have been conducted to investigate the removal efficiency of Cr(VI) ions from water by the PPy/BC composites. Shao et al.[25] prepared PPy/BC nanofiber composites by polymerizing pyrrole in the mixture with the fibrillated commercial nata de coco. The tested PPy/BC nanofiber composite displayed 37−99% removal efficiency in the pH range from 2 to 8. The pH dependence corresponded with the electrostatic attraction among positively charged nitrogen and chromium anion groups.[25] Marghaki et al.[26] prepared BC/Fe_3O_4/PPy sheets by coating magnetic BC sheets with PPy. The magnetic properties allowed BC/Fe_3O_4/PPy sheets to be separated from water using a magnet without filtration after metal ion adsorption. These magnetic sheets showed the removal efficiency of Cr(VI) from 47.65 to 99.25% at pH 3, depending on the adsorbent dosage. Both studies paid primary attention to the factors affecting the adsorption capacity values of BC/PPy composites. The present study extends the previous works by demonstrating that the free-standing BC/PPy composites enable a spontaneous electron transfer from PPy to Cr(VI) and, thus, leave only Cr(III) in the solution after reduction. The work also discusses the adsorption efficiency of BC/PPy composites of Cr(VI) and their viscoelastic properties, primarily with respect to the modification of wet or freeze-dried BC sheets. The possibility of using BC sheets in their natural wet form instead of dried sheets would reduce operation costs and preserve their fundamental physical properties.

2. EXPERIMENTAL SECTION

2.1. Materials. Yeast extract and peptone were provided by HiMedia (India). Citric acid anhydrous, disodium hydrogen phosphate dodecahydrate, glucose monohydrate, hydrochloric acid 37%, and sodium hydroxide were obtained from Penta (Czech Republic). Pyrrole, iron(III) chloride, potassium dichromate, and *N*,*N*-dimethylacetamide (DMAc) (≥99.0%) were purchased from Sigma-Aldrich (USA). Formic acid (98%) and lithium chloride were obtained from Lach-Ner (Czech Republic). All reagents used were of analytical grade.

2.2. Biosynthesis of BC. BC sheets were produced by static cultivation of *Komagataeibacter xylinus* (ATCC 53524) (Manassas, VA, USA) in a Hestrin−Schramm (HS) medium as reported elsewhere.[27] The HS medium was inoculated by a 7 day old bacterial suspension of 2×10^5 cfu mL^{-1}. The production cultivations were performed in 50 mL plastic tubes with a 38 mm diameter containing 20 mL of the HS medium (pH 5.1, 30 °C, stationary conditions, 14 days). BC sheets harvested from media were purified by treatment with 0.1 M NaOH at 80 °C for 90 min and then rinsed with distilled water until neutral pH was reached. The purified wet BC sheets were designated as BC/wet sheets and stored in 30% v/v ethanol at 4 °C. The freeze-dried samples were designated as BC/dry sheets.

2.3. Synthesis of BC/PPy Composites. BC/PPy composites were synthesized via in situ oxidative polymerization of pyrrole[28] (Figure 1). Prior to the synthesis, BC sheets were immersed in pyrrole for 24 h. 0.2 M pyrrole solution was oxidized with 0.5 M iron(III) chloride in the presence of pyrrole-soaked BC/wet or BC/dry sheets. The synthesis was conducted for 1 h at 20 °C and pH 1.8. The BC/PPy composites were then rinsed with 0.2 M HCl, cleaned with Mili-Q water until neutral pH, freeze-dried, and stored in closed containers. No filtration was needed since BC/PPy can be manually separated. The samples were designated as BC/wet/PPy and BC/dry/PPy composites, indicating the nature of BC used.

https://doi.org/10.1021/acsapm.4c00579
ACS Appl. Polym. Mater. XXXX, XXX, XXX−XXX

2.4. Characterization Techniques. FTIR spectra of freeze-dried BC sheets and BC/PPy composites were obtained by employing an attenuated total reflectance technique using a Thermo Nicolet NEXUS 870 spectrometer equipped with an MCT nitrogen-cooled detector (Thermo Fisher Scientific, Waltham, USA). IR spectra were recorded over 4000−650 cm^{-1} at 4 cm^{-1} resolution and represented an average of 256 scans.

The morphologies of freeze-dried BC sheets and BC/PPy composites were detected by scanning electron microscopy (MAIA3 Tescan, TESCAN, Brno, Czech Republic) at an acceleration voltage of 3.0 kV. Prior to the investigation, a 2 × 2 mm piece of each sample was placed on carbon tape and sputtered with gold particles.

The specific surface area (S_{BET}), pore volume (V_p), and pore size distribution of freeze-dried BC sheets and BC/PPy composites were determined by nitrogen adsorption−desorption (BET—Brunauer−Emmett−Teller) analyses using the nitrogen adsorption analyzer NOVA 2200e (Quantachrome Instruments, Boynton Beach, Florida, USA). Before measurement, the samples were degassed at 50 °C for 24 h.

The densities of freeze-dried BC sheets and BC/PPy composites were determined according to the standard test method ASTM D792-98, Method B.

The viscosity average molecular weight of BC was calculated by using the Mark−Houwink−Sakurada empirical equation. BC was dissolved in a LiCl/DMAc solvent system at 30 °C and the relative viscosity was determined using an Ubbelohde capillary viscometer.[29]

The swelling test was performed by immersing freeze-dried BC sheets and BC/PPy composites in acidic water (pH 3) at room temperature and mixing (200 rpm) for 48 h (pH and time span were chosen according to the conditions used for the adsorption experiments). The degree of swelling was calculated as follows

$$Q_{swell} = \frac{(W_S - W_D)}{W_D} \quad (1)$$

where W_S and W_D are the weights of the samples in the swelling state after 48 h and the dry state, respectively.

The thermal behavior of freeze-dried BC sheets and BC/PPy composites was investigated by thermogravimetric analysis (TGA) using a Pyris 1 thermogravimetric analyzer (PerkinElmer, New Castle, DE, USA). In the experiment, about 5 mg of the sample was heated from 30 to 800 °C at a heating rate of 10 °C min^{-1} in air.

The viscoelastic properties of BC/wet sheets and BC/wet/PPy and BC/dry/PPy composites were studied by small-amplitude oscillatory shear measurements using rotational rheometer DHR-2 (TA Instruments, Inc., USA). An 8 mm diameter sandblasted parallel plate was used measuring geometry with a gap between the plates adjusted to the sample thickness (about 1.0 mm). The amplitude (strain) sweep measurements were chosen to compare the viscoelastic properties of all of the tested samples. The oscillation frequency was maintained at a constant value of 1 Hz and the deformation amplitude was logarithmically increased from 0.05 to 1000% (logarithmic sweep, 6 points per decade). Prior to each measurement, the sample was swelled in water for 24 h and conditioned in a rheometer for 5 min at a constant temperature of 25 °C. The storage (G') and loss moduli (G'') were recorded.

2.5. Adsorption Experiments and Photocatalytic Reduction. The adsorption ability of BC/wet/PPy and BC/dry/PPy sheets was tested for the removal of Cr(VI) ions from aqueous solutions. Five milligrams of BC or BC/PPy were added to 25 mL of 50 mg L^{-1} of Cr(VI) solutions (pH 3). The mixtures were kept under mild shaking (200 rpm) at 23 ± 1 °C in the dark. The Cr(VI) concentration was followed with time by measuring the UV−visible spectra (Thermo Scientific, Evolution 220, Thermo Fisher, USA).

Adsorption capacity Q_e (mg g^{-1}) and removal efficiency (R %) were calculated according to the following formulas

$$Q_e = \frac{(C_i - C_e)}{m} \times V \quad (2)$$

$$R = \frac{(C_i - C_e)}{C_i} \times 100 \quad (3)$$

where C_i and C_e (mg L^{-1}) are the initial and equilibrium concentrations of Cr(VI), respectively. V (L) is the Cr(VI) solution volume and m (g) is the mass of the adsorbent.

The equilibrium isotherms were studied by mixing the adsorbents (5 mg) with a series of Cr(VI) solutions with different initial concentrations from 25 to 150 mg L^{-1} (25 mL; pH 3). The experiments were conducted at room temperature in dark conditions under gentle shaking (200 rpm). UV−visible spectra were collected at an equilibrium state after 48 h. Three different isotherm models, Langmuir, Freundlich, and Temkin, were used to study the equilibrium isotherms. The experimental data were fitted to linearized equations of isotherm models.[30]

Langmuir model

$$\frac{C_e}{Q_e} = \frac{1}{Q_{max}K_L} + \frac{C_e}{Q_{max}} \quad (4)$$

Freundlich model

$$\ln Q_e = \ln K_F + \frac{1}{n} \ln C_e \quad (5)$$

Temkin model

$$Q_e = b \ln K_T + b \ln C_e \quad (6)$$

where Q_{max} (mg g^{-1}) is the maximum adsorption capacity at saturation and K_L (L mg^{-1}) is the Langmuir constant. K_F (mg g^{-1}) is the Freundlich constant, which is related to the maximum adsorption capacity, and $1/n$ is a constant that describes the degree of nonlinearity between the Cr(VI) concentration and the adsorption process. K_T (L g^{-1}) is the Temkin isotherm constant, and b is a constant related to sorption heat. The best-fitting isotherm model was determined based on the linear regression coefficient (R^2) value.

The photocatalytic reduction of toxic Cr(VI) to nontoxic Cr(III) was conducted by using irradiation with warm white LED light (660 lm). Five milligrams of the BC/PPy sample were added to 25 mL of 50 mg L^{-1} of Cr(VI) aqueous solutions prepared in 1.0 M formic acid. Formic acid was used as a hole scavenger to enhance the photocatalytic reduction reaction.[31] UV−visible spectroscopy monitored the photocatalytic reduction of Cr(VI), measuring the absorbance at different time intervals. Additionally, inductively coupled plasma mass spectrometry (ICP-MS) (Nexion 2000 B, PerkinElmer, USA) was used to determine the total concentration of Cr(III) and Cr(VI) ions in the solutions after photocatalytic remediation experiments.

The selectivity of BC/PPy composites toward Cr(VI) ion adsorption was investigated in comparison with Cr(III), Co(II), and Cu(II); whereby BC/PPy composites (5 mg) were brought into contact with Cr(III) (50 mg/L; 25 mL) and a mixture of coexisting Cr(VI), Co(II), and Cu(II) (20 mg/L each; 25 mL) under the same conditions of Cr(VI) adsorption as before (pH 3, dark conditions, and 200 rpm). Different metal ion concentrations were determined at equilibrium after 48 h, using ICP-MS analysis.

At least three specimens were tested in each case of the experiment. One-way ANOVA using Origin (OriginPro 2019b) was applied to compare the statistical significance of the results. Differences among mean values were processed by the Tukey test at a level of significance of $p < 0.05$.

3. RESULTS AND DISCUSSION

3.1. Properties of BC/PPy Composites. The basis matrix for producing free-standing BC/PPy composites was biotechnologically produced BC with a viscosity average molecular weight of 462.4 kg mol^{-1} and density of 0.25 ± 0.03 g cm^{-3}. The biosynthesized BC membranes have characteristics suitable for water treatment applications, such as high purity, biocompatibility, versatility, and stable

https://doi.org/10.1021/acsapm.4c00579
ACS Appl. Polym. Mater. XXXX, XXX, XXX−XXX

mechanical properties.[32] The BC versatility enabled its modification with PPy. The production of BC/PPy composites consisted of adding wet or freeze-dried BC sheets in a pyrrole polymerization solution, which enabled the coating of PPy on the surface of BC. The BC/wet sheets were flexible and translucent white materials. In contrast, the BC/dry sheets were soft, brittle, and opaque white materials (Figure 1). After coating, BC/wet/PPy and BC/dry/PPy composites reached densities of 0.47 ± 0.02 and 0.30 ± 0.06 g cm^{-3}, respectively. Both types of BC sheets stayed as lightweight materials after PPy coating with slightly different structures. Table 1 displays

Table 1. Pore Characteristics Determined by BET Analysis

sample	surface area, S_{BET} (m^2 g^{-1})	pore volume, V_p (cm^3 g^{-1})
BC sheets	15.964	0.029
BC/dry/PPy	61.964	0.097
BC/wet/PPy	57.788	0.097

the pore characteristics. The coating of BC sheets with PPy enlarged the surface area of the composites. The modification of the specific surface area of BC/wet/PPy and BC/dry/PPy composites corresponds with the formation of new micropores and mesopores after the PPy coating (Figure S1a–c). Another advantage of free-standing BC/PPy composites is their easy handling due to their high flexibility and strength.

The synthesis of BC/PPy composites was verified by an ATR-FTIR analysis. Figure 2 displays the spectra of neat BC

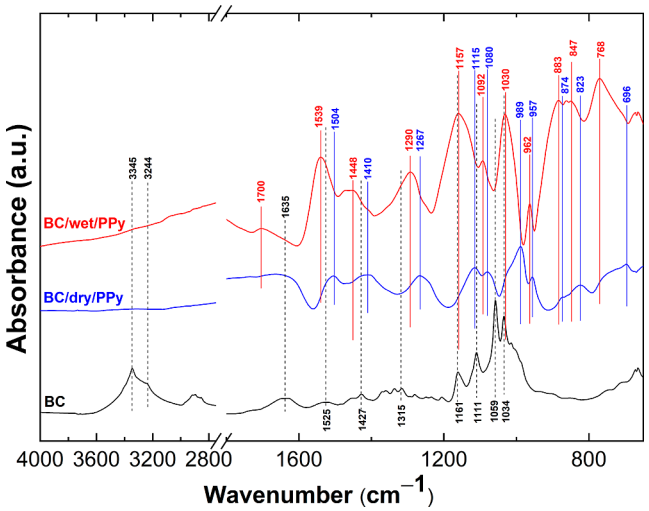

Figure 2. FTIR-ATR spectra of BC/dry sheets and BC/dry/PPy and BC/wet/PPy composites [color figure can be viewed in the online issue].

sheets and BC/PPy composites. The spectrum of neat BC sheets showed the characteristic peaks of cellulose at 1635 cm^{-1} (H–O–H bending of adsorbed water), 1525 cm^{-1} (C–H stretching), 1427 cm^{-1} (CH_2 bending or O–H in-plane bending), 1360 cm^{-1} (C–H deformation), 1315 cm^{-1} (O–H deformation), and in the region 1170–1030 cm^{-1} (C–O–C and C–O stretching deformation).[33,34] In addition, the determined peaks at 3345 and 3244 cm^{-1} are attributed to the hydrogen-bonded hydroxyl group (–OH) stretching vibration in cellulose.[35] FTIR spectra of both types of BC/PPy composites revealed the characteristic features of PPy in correspondence with the literature, with slight changes in the peak positions.[36,37] The BC/wet/PPy composite exhibited the characteristic peaks at 1539 cm^{-1} (C–C stretching in the ring of PPy), 1448 cm^{-1} (C–N stretching in the ring), 1290 cm^{-1} (C–N stretching), 1157 cm^{-1} (breathing vibration of the pyrrole ring), 1092 cm^{-1} ($N–H^+$ deformation vibration), 1030 cm^{-1} (C–H and N–H in-plane deformation vibrations), 962 cm^{-1} (C–C out-of-plane ring deformation), 883 cm^{-1} (N–H wagging of the PPy ring), 847 cm^{-1} (C–H and N–H out-of-plane bending), and 768 cm^{-1} (C–H out-of-plane ring deformations). The spectrum of BC/dry/PPy composites was red-shifted. The observed red shifts could occur due to hydrogen-bonding interaction between the N–H groups in the pyrrole rings and the lone pair of electrons on the oxygen atoms of the hydroxyl groups on the cellulose surface.[33] In accordance with the ATR-FTIR method, a surface-sensitive technique, only PPy characteristic peaks were identified on the surface of both types of BC/PPy composites. It confirms the successful coating of the BC sheets by PPy during the polymerization.

The microstructures of neat BC sheets and BC/PPy composites were investigated by using SEM (Figures 3 and 4). The BC/dry sheets formed a coherent 3D network composed of cellulose fibers, as shown in Figures 3a and 4a. The BC/dry/PPy composites displayed microfibrils forming clusters (Figures 3b and 4b). In contrast, the BC/wet/PPy composites exhibited separated ribbon-like microfibrils launching in highly fibrous structures (Figures 3c and 4c).

The SEM-EDX elemental mapping spectra of BC/dry/PPy and BC/wet/PPy composites (Figure S2b,c) confirmed the successful coating of BC by PPy during the polymerization. The spectra of the coated sheets compared to those of neat BC sheets (Figure S2a) proved an increased nitrogen content from 6 to 17 wt %.

The BC used for modification by the PPy coating was wet (BC/wet/PPy) or dried (BC/dry/PPy). As the cellulose absorbs water, it undergoes volume expansion due to the penetration of water molecules into its structure. Swelling leads to an increase in the surface area of the cellulose.[38] On the grounds that the swelling degree may be connected with the thermal stability of samples as well as the adsorption capacity of metal ions, the swelling degree of neat BC sheets and BC/PPy composites was determined. The swelling properties of dry composites were evaluated under the same conditions as those used for later adsorption experiments (pH 3, 200 rpm, 48 h). The neat BC sheets exhibited a swelling degree of 46.9 ± 0.4 after 48 h. BC/wet/PPy and BC/dry/PPy composites demonstrated much lower swelling degrees of 21.9 ± 0.3 and 22.4 ± 2.1, respectively. The resulting swelling degrees of both BC/PPy composites were similar, indicating a negligible effect of the BC state (dry or wet) on the swelling behavior of the PPy-coated BC composites.

The thermal stability of dry BC/PPy composites in dependence on the BC state used for modification was studied by TGA (Figure S3). The TGA spectrum of the neat BC sheets revealed thermal degradation steps typical for the cellulose.[39] The thermal stability of BC was considerably improved after PPy coating, mainly when wet cellulose was used. The lower thermal stability of neat BC may be partially connected to its higher swelling ability than BC/PPy composites. There are some possible explanations: (1) due to the higher swelling ability of BC compared to BC/PPy composites, dry BC sheets may contain more bound water also in the dry form that, finally, led to lower thermal stability and

https://doi.org/10.1021/acsapm.4c00579
ACS Appl. Polym. Mater. XXXX, XXX, XXX–XXX

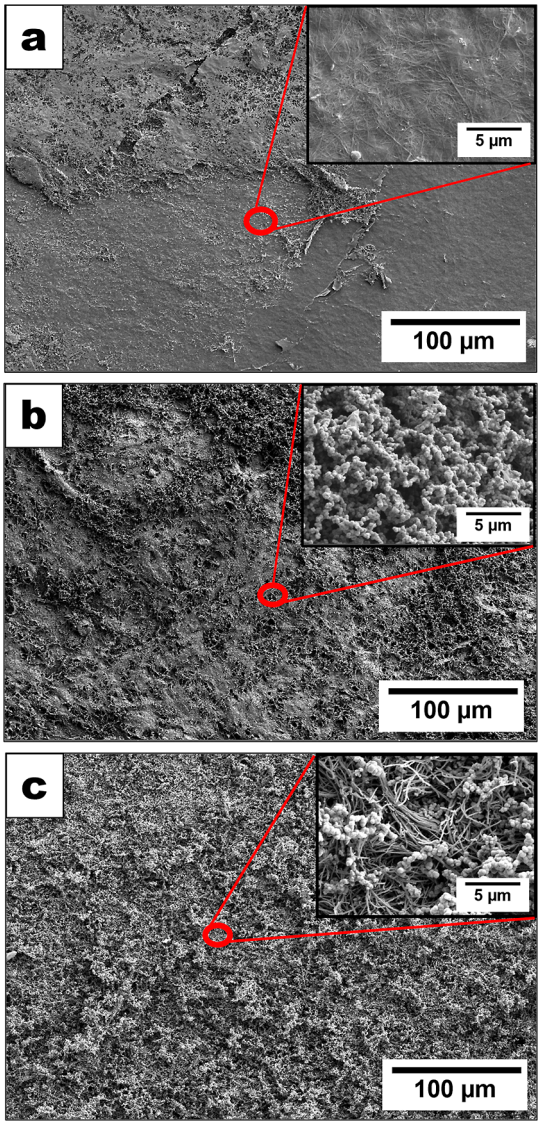

Figure 3. SEM micrographs of (a) BC/dry sheet, (b) BC/dry/PPy composites, and (c) BC/wet/PPy composites.

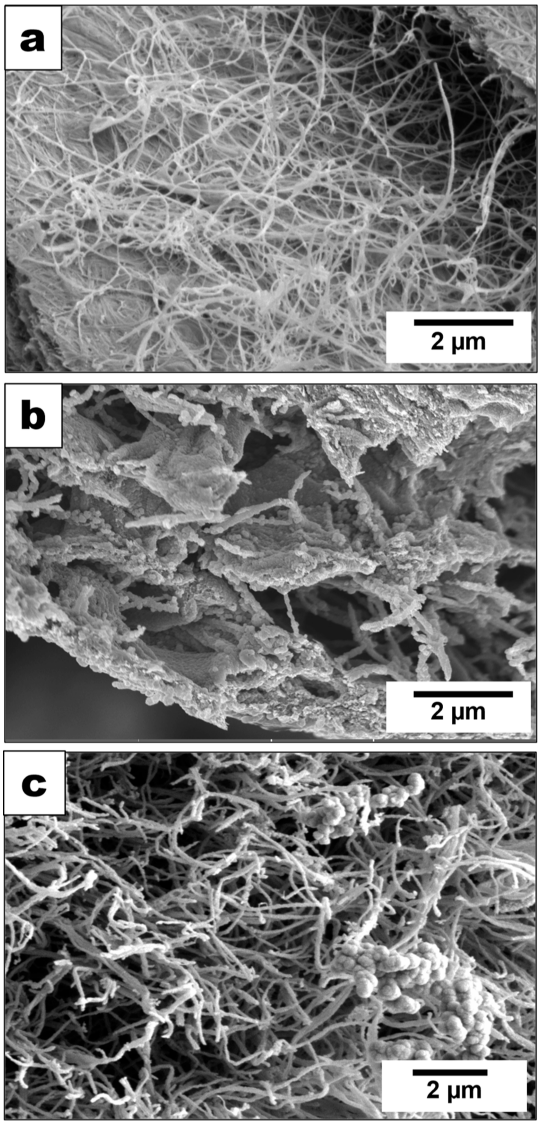

Figure 4. Cross-sectional morphologies of (a) BC/dry sheet, (b) BC/dry/PPy, and (c) BC/wet/PPy composites.

(2) the morphology of dry BC enabled even dry samples to absorb water from the environment very quickly. The TGA spectra of BC/PPy composites compared to neat BC sheets displayed only two degradation steps, indicating the loss of moisture at ∼100 °C and the degradation of composites starting at 260 °C and ending at 550 or 643 °C, depending on the nature of coated BC (dry or wet). The detected start of the degradation of BC/PPy composites at 260 °C may be related to the release of the residual protonating acid and the degradation of the sample. The complete decomposition of the neat BC sheets occurred at about 600 °C with a residue of 5.7 wt %. The BC/dry/PPy and BC/wet/PPy composites left about 0.7−1.8 times higher residues. The higher amounts of BC/PPy composite residues correspond with the presence of iron oxides produced from the oxidant during polymerization. The thermal stability of the samples increased in the order of BC/dry sheet < BC/dry/PPy composite < BC/wet/PPy composite. The determined high thermal stability of BC/wet/PPy composites may indicate the elimination of the negative impact of BC drying before PPy coating.

Viscoelastic properties were examined due to the apparent change in the mechanical integrity of BC/PPy composites from the view of higher brittleness in the case of BC/dry/PPy composites compared to the BC/wet/PPy composites. Figure 5 shows the storage (G') and loss (G'') moduli as a function of oscillation strain. All tested samples at a low deformation amplitude in the linear viscoelastic region (LVER) reached larger G' than G'', indicating viscoelastic behavior with a predominance of elasticity. The amplitude sweep measurements provided essential information about the strength of interactions in the inner structure of BC sheets and BC/PPy composites. The end of the LVER was evaluated. LVER is the point at which the value of the complex modulus exceeds more than 5% of its original value.[40] The BC/wet/PPy composites exhibited the most extended viscoelastic region compared with BC dry sheets and BC/dry/PPy composites. It indicates that the coating of wet BC sheets by PPy resulted in a more persistent composite in the strain before the deformation than in the coating of dry BC sheets. Thus, it may be claimed that the viscoelastic properties of BC/PPy composites can be

https://doi.org/10.1021/acsapm.4c00579
ACS Appl. Polym. Mater. XXXX, XXX, XXX−XXX

regulated by selecting the BC nature (wet or dry) for PPy coating.

3.2. Adsorption and Photocatalytic Reduction of Cr(VI). The Cr(VI) adsorption capacities of BC/dry sheets and BC/PPy composites were investigated at pH 3 in the dark (without access to light irradiation). Based on the literature and our previous results, the highest removal efficiency of Cr(VI) occurs in the environment of pH 3 due to the favorable valence states of chromate in the form of $HCrO_4^-$.[34,41] Time-dependent UV−visible spectra of Cr(VI) ions after adsorption on neat BC sheets and BC/PPy composites are shown in Figure 6a−c. As expected, the neat BC/dry sheet exhibited a low affinity for Cr(VI) ions (Figure 6a). The adsorption capacity of BC significantly increased after coating with PPy (Figure 6b,c). The electrostatic interaction of positively charged PPy chains with $HCrO_4^-$ ions was experimentally detectable by the gradual slow fading of the yellow color of the Cr(VI) solution. The adsorption process was much faster at the beginning of the adsorption process due to the free available surface binding sites on the BC/PPy composites. However, after gradual saturation of the active sorption sites, the adsorption slowed considerably to a complete stop of the adsorption after the equilibrium point was reached. The continuous and smooth time-dependent adsorption plots suggest monolayer adsorption of Cr(VI) onto the surface of BC/PPy composites.[42,43] Both BC/dry/PPy and BC/wet/PPy composites reached comparable values of the removal efficiency of about 88% and adsorption capacity of about 220 mg g^{-1} after 48 h (Figure 6d). The relatively slow adsorption rate can be assigned to the tightly packed and compact morphology of the BC/PPy composites (Figure 3).

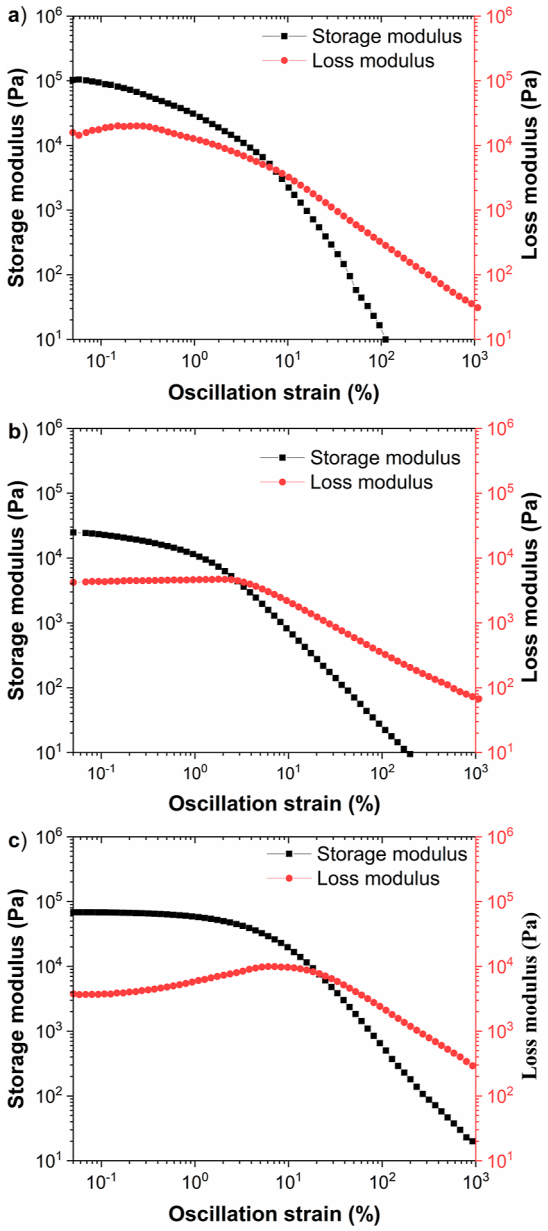

Figure 5. Strain dependence of storage and loss moduli obtained for (a) BC/dry sheets and (b) BC/dry/PPy and (c) BC/wet/PPy composites [color figure can be viewed in the online issue].

The affinity of BC/PPy composites to Cr(VI) ions and adsorption mechanisms were evaluated using Langmuir, Freundlich, and Temkin models (Figures S4−S6).[44] Isotherm parameters summarized in Table 2 show that the Langmuir model best fits the Cr(VI) adsorption experimental data for both BC/PPy composites. This indicates that the adsorption of Cr(VI) ions occurs as a homogeneous monolayer on the surface of BC/PPy composites. The Langmuir maximum adsorption capacity was about 294 and 286 mg g^{-1} for BC/dry/PPy and BC/wet/PPy composites, respectively. These composites have demonstrated a relatively high maximum adsorption capacity compared with other previously published cellulose-based PPy composites (Table S1). Langmuir constant (K_L) values were similar for both types of composites, which could assume a similar extent of surface interaction with Cr(VI) ions in the case of using BC/dry/PPy and BC/wet/PPy composites. From the Freundlich model fitting, the values of $1/n$ predict a favorable adsorption process of Cr(VI) on both BC/PPy composites in the range of $0.1 < 1/n < 1$. Temkin isotherms described the heat energy of adsorption due to the Cr(VI) ion and BC/PPy composite interactions.[43] Temkin constants b were 93.5 and 85.4 J mol^{-1} for BC/PPy composites prepared under dry and wet conditions, which might indicate a chemisorption process. The adsorption affinities determined for both types of BC/PPy composites are comparable without the influence of the original nature of BC used for coating by PPy.

The composites of BC/PPy have shown high selectivity toward Cr(VI) ions when compared to Cr(III) ions or the coexisting Co(II) and Cu(II) heavy metal ions. The results reveal the high selectivity of Cr(VI) to be adsorbed onto BC/PPy composites in comparison with Cr(III) and the coexisting Co(II) and Cu(II), which have shown no affinity toward BC/PPy composites as presented in Figure S7.

In this work, BC/PPy composites were further tested as catalysts for their ability to reduce Cr(VI) ions photocatalytically under visible-light irradiation. Figure 7a,b shows the time dependence of Cr(VI) absorbance after exposure to LED light. The characteristic peak of Cr(VI) at 350 nm decreased linearly with time, with a Cr(VI) removal efficiency of 96.8 and 97.3% after 14 h when using BC/wet/PPy and BC/dry/PPy composites, respectively, compared to 80.9 and 79.8% of Cr(VI) removed after 24 h by adsorption (Figure S8). Figure 7c shows the dependence of the Cr(VI) ion concentration on the photocatalytic reduction time up to 24 h. In addition, the Cr(VI) solutions after the photocatalytic reduction with LED were analyzed by ICP-MS to determine the concentration of Cr(III) ions. The determined concentrations of Cr(III) ions

https://doi.org/10.1021/acsapm.4c00579
ACS Appl. Polym. Mater. XXXX, XXX, XXX−XXX

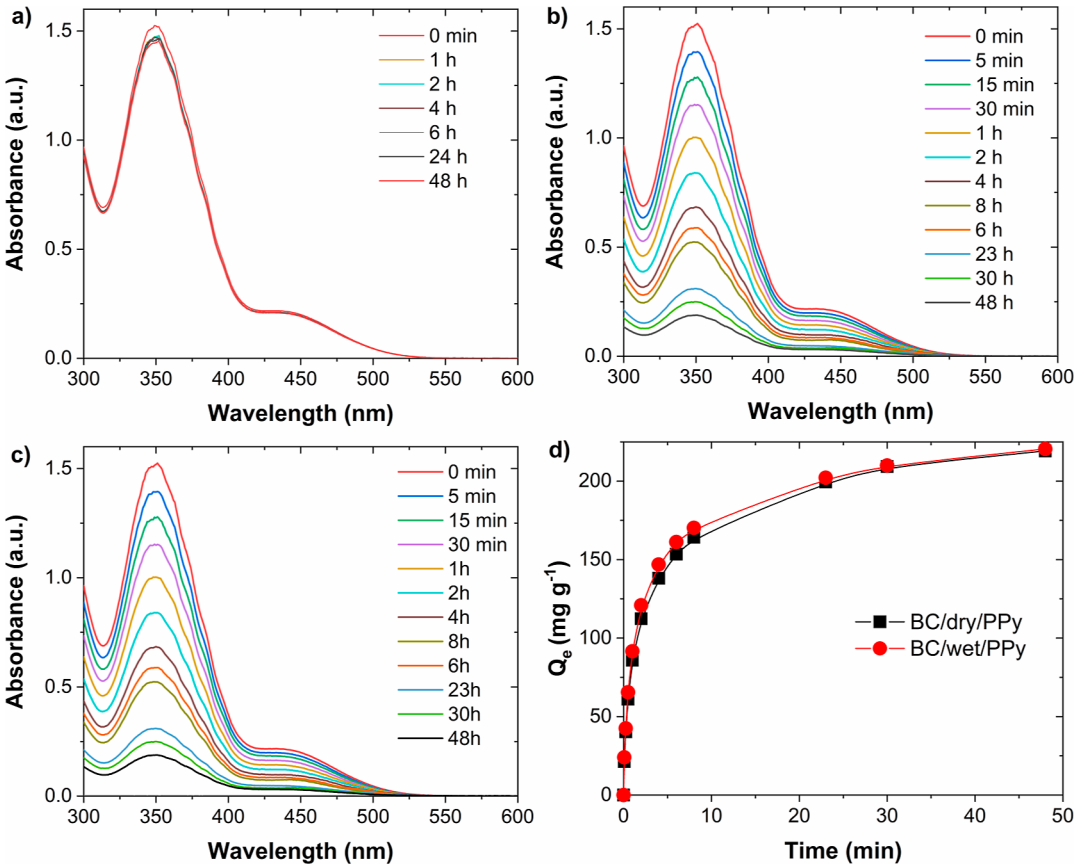

Figure 6. Time-dependent UV−visible spectra of Cr(VI) ions in solutions (50 mg L^{-1}) after adsorption onto (a) BC/dry sheet, (b) BC/dry/PPy composites, and (c) BC/wet/PPy composites; and (d) time-dependent adsorption capacity (Q_e) of BC/PPy composites [color figure can be viewed in the online issue].

Table 2. Equilibrium Isotherm Model Parameters[a]

adsorbent	Langmuir model			Freundlich model			Temkin model		
	Q_{max}, (mg g^{-1})	K_L, (L mg^{-1})	R^2	K_F, (mg g^{-1})	$1/n$	R^2	K_T, (L g^{-1})	b, (J mol^{-1})	R^2
BC/dry/PPy	294.1 ± 9.3[a]	0.326 ± 0.0001[a]	0.997	154.5 ± 3.26[a]	0.139 ± 0.0064[a]	0.994	447.6 ± 136.4[a]	26.52 ± 2.48[a]	0.974
BC/wet/PPy	285.7 ± 8.2[a]	0.206 ± 0.018[b]	0.998	163.7 ± 11.6[a]	0.147 ± 0.023[a]	0.934	395.1 ± 188.5[a]	29.20 ± 4.44[a]	0.934

[a]Data presented as mean value ± standard deviation. Values for each sample with different superscripts (a and b) are significantly different ($p < 0.05$).

were 36.1 ± 1.6 and 34.8 ± 1.1 mg L^{-1} for the BC/dry/PPy and BC/wet/PPy membranes, respectively. Around 69.5 and 72.0% of the treated Cr(VI) were converted into Cr(III) using BC/wet/PPy and BC/dry/PPy, respectively. Only 28.9 and 26.7% of Cr(VI) were adsorbed onto BC/wet/PPy and BC/dry/PPy, respectively, during the photocatalytic reduction process. This confirmed that due to the low affinity between BC/PPy composites and most Cr(III) ions, Cr(III) was released back to the solution from the membranes' surfaces of BC/PPy composites after reduction takes place.

The extent of the catalytic reduction of Cr(VI) was evaluated by using the following first-order kinetics[45]

$$\ln(C_t/C_0) = -k_{app}t \quad (7)$$

where C_0 (mg L^{-1}) is the initial Cr(VI) concentration, C_t (mg L^{-1}) is the concentration at time t (min), and k_{app} (min^{-1}) is the apparent rate constant.

Figure 7d shows a linear correlation between $\ln(C_t/C_0)$ and the photocatalytic exposition reduction time. The obtained data confirmed that the photocatalytic reduction reaction followed first-order kinetics. The apparent rate constant (k_{app}) was calculated to be 8.6×10^{-3} and 8.8×10^{-3} min^{-1} for BC/dry/PPy and BC/wet//PPy composites, respectively.

Based on the results, it can be concluded that both types of BC/PPy free-standing composites are very efficient for the reduction of Cr(VI) ions. The direct use of wet BC sheets for PPy coating has a great advantage, such as time savings and lower operation costs from the point of omitted freeze-drying step with a final high reduction efficiency of Cr(VI) to Cr(III).

4. CONCLUSIONS

We demonstrated that wet and dry BC sheets may serve as a matrix for preparing BC/PPy composites with high adsorption affinity for hexavalent chromium. Free-standing BC/dry/PPy and BC/wet/PPy composites were prepared by polymerizing pyrrole in the presence of BC sheets. Both types of BC/PPy composites were lightweight materials with a density of 0.30−0.47 g cm^{-3} and markedly improved thermal stability compared to neat BC sheets. The viscoelastic properties of BC/PPy composites depended on the nature of BC used for

https://doi.org/10.1021/acsapm.4c00579
ACS Appl. Polym. Mater. XXXX, XXX, XXX−XXX

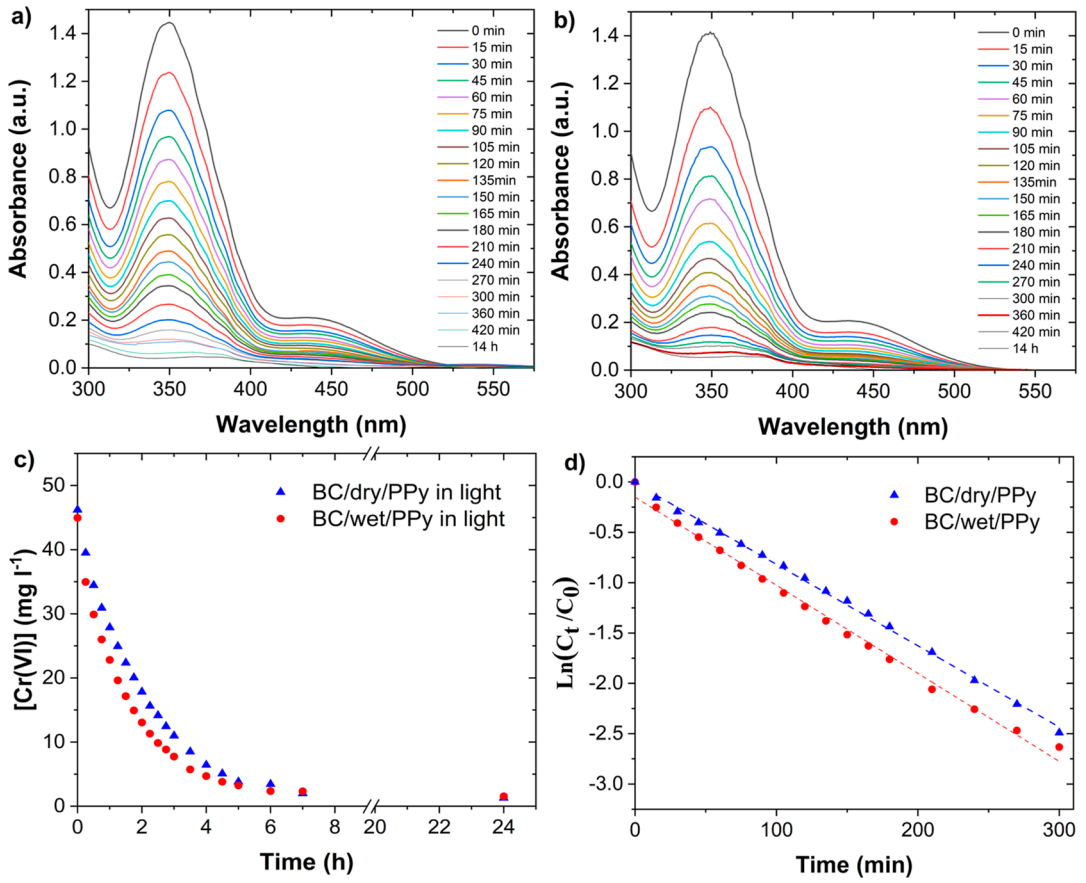

Figure 7. Time-dependent UV−visible spectra of Cr(VI) solutions during photocatalytic reduction (exposed to LED warm light) using (a) BC/dry/PPy and (b) BC/wet/PPy composites; (c) dependence of Cr(VI) ion concentration on the exposition reduction time, and (d) dependence of $\ln(C_t/C_0)$ on the exposition reduction time [color figure can be viewed in the online issue].

the coating. The modification of wet BC supported the higher mechanical integrity of the BC/wet/PPy composite compared to the BC/dry/PPy composite. The BC/PPy composites were tested as templates for removing hexavalent chromium ions from an aqueous solution. When fitting the experimental data using the Langmuir, Freundlich, and Temkin models, the Langmuir model was found to be the best fit. This confirms that Cr(VI) ions were predominantly bound to the BC/PPy surface interface. Both types of the BC/PPy composites reached comparable adsorption capacities, approximately 294 mg g^{-1} at 23 °C and dark conditions. Similarly, these composites could effectively reduce toxic Cr(VI) to nontoxic Cr(III) ions in aqueous solutions.

The findings of this study confirmed that the use of free-standing BC/wet/PPy composites to remove hexavalent chromium ions from polluted water is an environmentally friendly and effective method. The advantage of this method is the direct modification of wet BC (without the drying step), resulting in free-standing and mechanically stable BC/wet/PPy composites. Applying free-standing BC/wet/PPy composites after adsorption/reduction of the hexavalent chromium ions does not require water filtration for the final entrapment of the BC/PPy composites.

■ ASSOCIATED CONTENT

Supporting Information

The Supporting Information is available free of charge at https://pubs.acs.org/doi/10.1021/acsapm.4c00579.

Pore size distribution, EDX spectrum, TGA, Langmuir isotherms, Freundlich isotherms, Temkin isotherms, removal efficiency of various heavy metal ions by Cr(VI) by BC/PPy composites, time-dependent removal efficiency of Cr(VI) by BC/PPy composites, and Cr(VI) ion adsorption capacity of different cellulose-based PPy composites (PDF)

■ AUTHOR INFORMATION

Corresponding Author

Adriana Kovalcik − *Faculty of Chemistry, Brno University of Technology, 612 00 Brno, Czech Republic;* orcid.org/0000-0003-4833-7369; Email: kovalcik@fch.vut.cz

Authors

Radim Striz − *Faculty of Chemistry, Brno University of Technology, 612 00 Brno, Czech Republic;* orcid.org/0009-0005-1316-7154

Islam M. Minisy − *Institute of Macromolecular Chemistry, Czech Academy of Sciences, 162 00 Prague, Czech Republic;* orcid.org/0000-0001-5785-1787

Patrycja Bober − *Institute of Macromolecular Chemistry, Czech Academy of Sciences, 162 00 Prague, Czech Republic;* orcid.org/0000-0002-1667-8604

Oumayma Taboubi − *Institute of Macromolecular Chemistry, Czech Academy of Sciences, 162 00 Prague, Czech Republic*

Jiří Smilek − *Faculty of Chemistry, Brno University of Technology, 612 00 Brno, Czech Republic*

https://doi.org/10.1021/acsapm.4c00579
ACS Appl. Polym. Mater. XXXX, XXX, XXX−XXX

Complete contact information is available at:
https://pubs.acs.org/10.1021/acsapm.4c00579

Author Contributions

R.S.: Investigation, visualization, and writing—original draft. **I.M.M.**: Investigation, methodology, and writing—review and editing. **P.B.**: Conceptualization, validation, and writing—review and editing. **O.T.**: Investigation and writing—review and editing. **J.S.**: Investigation and validation. **A.K.**: Conceptualization, supervision, validation, and writing—original draft, review, and editing.

Notes

The authors declare no competing financial interest.

■ ACKNOWLEDGMENTS

R.S. and A.K. acknowledge funding through the internal scientific grant of Brno University of Technology (FCH-S-23-8330). I.M.M. and P.B. thank the Czech Science Foundation (21-01401S). Moreover, the authors thank Ms. J. Hromádková for providing the SEM/EDAX measurements and Ing. Vladislav Caba for BET analysis.

■ REFERENCES

(1) Bisselink, B.; B, J.; Gelati, E.; Adamovic, M.; Guenther, S.; Mentaschi, L.; Feyen, L.; de Roo, A. *Climate Change and Europe's Water Resources*; Publications Office of the European Union, 2020.
(2) Rathi, B. S.; Kumar, P. S.; Vo, D.-V. N. Critical review on hazardous pollutants in water environment: Occurrence, monitoring, fate, removal technologies and risk assessment. *Sci. Total Environ.* **2021**, *797*, 149134.
(3) Arora, N. K.; Chauhan, R. Heavy metal toxicity and sustainable interventions for their decontamination. *Environ. Sustainability* **2021**, *4* (1), 1−3.
(4) Bolisetty, S.; Peydayesh, M.; Mezzenga, R. Sustainable technologies for water purification from heavy metals: review and analysis. *Chem. Soc. Rev.* **2019**, *48* (2), 463−487.
(5) Chromium in drinking-water. *Background Document for Development of WHO Guidelines for Drinking-Water Quality*. World Health Organization: Geneva, 2020.
(6) *Directive (EU) 2020/2184 of the European PArliament and of the Council of 16 December 2020 on the Quality of Water Intended for Human Consumption*, 2020. https://eur-lex.europa.eu/eli/dir/2020/2184/oj (accessed Dec 23, 2020).
(7) Karimi-Maleh, H.; Ayati, A.; Ghanbari, S.; Orooji, Y.; Tanhaei, B.; Karimi, F.; Alizadeh, M.; Rouhi, J.; Fu, L.; Sillanpää, M. Recent advances in removal techniques of Cr (VI) toxic ion from aqueous solution: a comprehensive review. *J. Mol. Liq.* **2021**, *329*, 115062.
(8) Smol, M.; Prasad, M. N. V.; Stefanakis, A. I. *Water in Circular Economy*; Springer Nature: Switzerland AG, 2023; .
(9) Jiang, X.; Li, Y.; Tang, X.; Jiang, J.; He, Q.; Xiong, Z.; Zheng, H. Biopolymer-based flocculants: A review of recent technologies. *Environ. Sci. Pollut. Res.* **2021**, *28*, 46934−46963.
(10) Guo, D.-M.; An, Q.-D.; Xiao, Z.-Y.; Zhai, S.-R.; Shi, Z. Polyethylenimine-functionalized cellulose aerogel beads for efficient dynamic removal of chromium (VI) from aqueous solution. *RSC Adv.* **2017**, *7* (85), 54039−54052.
(11) Yang, C.; Yang, H.-R.; An, Q.-D.; Xiao, Z.-Y.; Zhai, S.-R. Recyclable CMC/PVA/MIL-101 aerogels with tailored network and affinity sites for efficient heavy metal ions capture. *Chem. Eng. J.* **2022**, *447*, 137483.
(12) Yang, H.-R.; Yang, C.; Li, S.-S.; Shan, X.-C.; Song, G.-L.; An, Q.-D.; Zhai, S.-R.; Xiao, Z.-Y. Site-imprinted hollow composites with integrated functions for ultra-efficient capture of hexavalent chromium from water. *Sep. Purif. Technol.* **2022**, *284*, 120240.
(13) Hussain, Z.; Sajjad, W.; Khan, T.; Wahid, F. Production of bacterial cellulose from industrial wastes: a review. *Cellulose* **2019**, *26*, 2895−2911.
(14) Abeer, M. M.; Mohd Amin, M. C. I.; Martin, C. A review of bacterial cellulose-based drug delivery systems: their biochemistry, current approaches and future prospects. *J. Pharm. Pharmacol.* **2014**, *66* (8), 1047−1061.
(15) Ciecholewska-Juśko, D.; Broda, M.; Żywicka, A.; Styburski, D.; Sobolewski, P.; Gorący, K.; Migdał, P.; Junka, A.; Fijałkowski, K. Potato juice, a starch industry waste, as a cost-effective medium for the biosynthesis of bacterial cellulose. *Int. J. Mol. Sci.* **2021**, *22* (19), 10807.
(16) Blanco Parte, F. G.; Santoso, S. P.; Chou, C.-C.; Verma, V.; Wang, H.-T.; Ismadji, S.; Cheng, K.-C. Current progress on the production, modification, and applications of bacterial cellulose. *Crit. Rev. Biotechnol.* **2020**, *40* (3), 397−414.
(17) Hur, D. H.; Choi, W. S.; Kim, T. Y.; Lee, S. Y.; Park, J. H.; Jeong, K. J. Enhanced production of bacterial cellulose in Komagataeibacter xylinus via tuning of biosynthesis genes with synthetic RBS. *J. Microbiol. Biotechnol.* **2020**, *30* (9), 1430−1435.
(18) Amason, A.-C.; Meduri, A.; Rao, S.; Leonick, N.; Subramaniam, B.; Samuel, J.; Gross, R. A. Bacterial Cellulose Cultivations Containing Gelatin Form Tunable, Highly Ordered, Laminae Structures with Fourfold Enhanced Productivity. *ACS omega* **2022**, *7* (51), 47709−47719.
(19) Fijałkowski, K.; Żywicka, A.; Drozd, R.; Junka, A. F.; Peitler, D.; Kordas, M.; Konopacki, M.; Szymczyk, P.; El Fray, M.; Rakoczy, R. Increased yield and selected properties of bacterial cellulose exposed to different modes of a rotating magnetic field. *Eng. Life Sci.* **2016**, *16* (5), 483−493.
(20) Mohite, B. V.; Koli, S. H.; Patil, S. V. Bacterial Cellulose-Based Hydrogels: Synthesis, Properties, and Applications. In *Cellulose-Based Superabsorbent Hydrogels*; Mondal, M. I. H., Ed.; Springer International Publishing, 2019; pp 1255−1276.
(21) Ahmaruzzaman, M.; Roy, P.; Bonilla-Petriciolet, A.; Badawi, M.; Ganachari, S. V.; Shetti, N. P.; Aminabhavi, T. M. Polymeric hydrogels-based materials for wastewater treatment. *Chemosphere* **2023**, *331*, 138743.
(22) Stejskal, J. Conducting polymers are not just conducting: a perspective for emerging technology. *Polym. Int.* **2020**, *69* (8), 662−664.
(23) Taghizadeh, A.; Taghizadeh, M.; Jouyandeh, M.; Yazdi, M. K.; Zarrintaj, P.; Saeb, M. R.; Lima, E. C.; Gupta, V. K. Conductive polymers in water treatment: A review. *J. Mol. Liq.* **2020**, *312*, 113447.
(24) Roy, K.; Mondal, P.; Bayen, S.; Chowdhury, P. Sonochemical synthesis of polypyrrole salt and study of its Cr (VI) sorption-desorption properties. *J. Macromol. Sci., Part A* **2012**, *49* (11), 931−935.
(25) Shao, Y.; Fan, Z.; Zhong, M.; Xu, W.; He, C.; Zhang, Z. Polypyrrole/bacterial cellulose nanofiber composites for hexavalent chromium removal. *Cellulose* **2021**, *28* (4), 2229−2240.
(26) Marghaki, N. S.; Jonoush, Z. A.; Rezaee, A. Chromium (VI) removal using microbial cellulose/nano-Fe3O4@ polypyrrole: isotherm, kinetic and thermodynamic studies. *Mater. Chem. Phys.* **2022**, *278*, 125696.
(27) Fijałkowski, K.; Żywicka, A.; Drozd, R.; Niemczyk, A.; Junka, A. F.; Peitler, D.; Kordas, M.; Konopacki, M.; Szymczyk, P.; Fray, M. E.; Rakoczy, R. Modification of bacterial cellulose through exposure to the rotating magnetic field. *Carbohydr. Polym.* **2015**, *133*, 52−60.
(28) Sapurina, I.; Li, Y.; Alekseeva, E.; Bober, P.; Trchová, M.; Morávková, Z.; Stejskal, J. Polypyrrole nanotubes: the tuning of morphology and conductivity. *Polymer* **2017**, *113*, 247−258.
(29) McCormick, C. L.; Callais, P. A.; Hutchinson, B. H. Solution studies of cellulose in lithium chloride and N, N-dimethylacetamide. *Macromolecules* **1985**, *18* (12), 2394−2401.
(30) Minisy, I. M.; Salahuddin, N. A.; Ayad, M. M. Adsorption of methylene blue onto chitosan-montmorillonite/polyaniline nanocomposite. *Appl. Clay Sci.* **2021**, *203*, 105993.

(31) Islam, J. B.; Furukawa, M.; Tateishi, I.; Katsumata, H.; Kaneco, S. Photocatalytic reduction of hexavalent chromium with nanosized TiO2 in presence of formic acid. *ChemEngineering* **2019**, *3* (2), 33.
(32) Liu, W.; Du, H.; Zhang, M.; Liu, K.; Liu, H.; Xie, H.; Zhang, X.; Si, C. Bacterial cellulose-based composite scaffolds for biomedical applications: a review. *ACS Sustainable Chem. Eng.* **2020**, *8* (20), 7536−7562.
(33) Bober, P.; Liu, J.; Mikkonen, K. S.; Ihalainen, P.; Pesonen, M.; Plumed-Ferrer, C.; von Wright, A.; Lindfors, T.; Xu, C.; Latonen, R.-M. Biocomposites of nanofibrillated cellulose, polypyrrole, and silver nanoparticles with electroconductive and antimicrobial properties. *Biomacromolecules* **2014**, *15* (10), 3655−3663.
(34) Minisy, I. M.; Acharya, U.; Veigel, S.; Morávková, Z.; Taboubi, O.; Hodan, J.; Breitenbach, S.; Unterweger, C.; Gindl-Altmutter, W.; Bober, P. Sponge-like polypyrrole-nanofibrillated cellulose aerogels: synthesis and application. *J. Mater. Chem. C* **2021**, *9* (37), 12615−12623.
(35) Somord, K.; Somord, K.; Suwantong, O.; Thanomsilp, C.; Peijs, T.; Soykeabkaew, N. Self-reinforced poly (lactic acid) nanocomposites with integrated bacterial cellulose and its surface modification. *Nanocomposites* **2018**, *4* (3), 102−111.
(36) Acharya, U.; Bober, P.; Trchová, M.; Zhigunov, A.; Stejskal, J.; Pfleger, J. Synergistic conductivity increase in polypyrrole/molybdenum disulfide composite. *Polymer* **2018**, *150*, 130−137.
(37) Stejskal, J.; Trchová, M.; Bober, P.; Morávková, Z.; Kopecký, D.; Vrňata, M.; Prokeš, J.; Varga, M.; Watzlová, E. Polypyrrole salts and bases: superior conductivity of nanotubes and their stability towards the loss of conductivity by deprotonation. *RSC Adv.* **2016**, *6* (91), 88382−88391.
(38) Hribernik, S.; Stana Kleinschek, K.; Rihm, R.; Ganster, J.; Fink, H.-P.; Sfiligoj Smole, M. Tuning of cellulose fibres' structure and surface topography: Influence of swelling and various drying procedures. *Carbohydr. Polym.* **2016**, *148*, 227−235.
(39) Jahan, F.; Kumar, V.; Saxena, R. K. Distillery effluent as a potential medium for bacterial cellulose production: A biopolymer of great commercial importance. *Bioresour. Technol.* **2018**, *250*, 922−926.
(40) Trudicova, M.; Smilek, J.; Kalina, M.; Smilkova, M.; Adamkova, K.; Hrubanova, K.; Krzyzanek, V.; Sedlacek, P. Multiscale experimental evaluation of agarose-based semi-interpenetrating polymer network hydrogels as materials with tunable rheological and transport performance. *Polymers (Basel)* **2020**, *12* (11), 2561.
(41) Kong, F.; Zhang, Y.; Wang, H.; Tang, J.; Li, Y.; Wang, S. Removal of Cr(VI) from wastewater by artificial zeolite spheres loaded with nano Fe-Al bimetallic oxide in constructed wetland. *Chemosphere* **2020**, *257*, 127224.
(42) Bober, P.; Minisy, I. M.; Morávková, Z.; Hlídková, H.; Hodan, J.; Hromádková, J.; Acharya, U. Polypyrrole Aerogels: Efficient Adsorbents of Cr (VI) Ions from Aqueous Solutions. *Gels* **2023**, *9* (7), 582.
(43) Karthikeyan, T.; Rajgopal, S.; Miranda, L. R. Chromium(VI) adsorption from aqueous solution by sawdust activated carbon. *J. Hazard. Mater.* **2005**, *124* (1−3), 192−199.
(44) Piccin, J. S.; Vieira, M.; Gonçalves, J.; Dotto, G.; Pinto, L. A. d. A. Adsorption of FD&C Red No. 40 by chitosan: Isotherms analysis. *J. Food Eng.* **2009**, *95* (1), 16−20.
(45) Minisy, I. M.; Taboubi, O.; Hromádková, J. One-Step Accelerated Synthesis of Conducting Polymer/Silver Composites and Their Catalytic Reduction of Cr (VI) Ions and p-Nitrophenol. *Polymers* **2023**, *15* (10), 2366.

https://doi.org/10.1021/acsapm.4c00579
ACS Appl. Polym. Mater. XXXX, XXX, XXX−XXX